APL Materials

High-mobility $BaSnO_3$ grown by oxide molecular beam epitaxy

Cite as: APL Mater. 4, 016106 (2016); https://doi.org/10.1063/1.4939657
Submitted: 13 October 2015 • Accepted: 26 December 2015 • Published Online: 28 January 2016

Santosh Raghavan, Timo Schumann, Honggyu Kim, et al.

APL MATERIALS **4**, 016106 (2016)

High-mobility $BaSnO_3$ grown by oxide molecular beam epitaxy

Santosh Raghavan,[a] Timo Schumann,[a] Honggyu Kim, Jack Y. Zhang, Tyler A. Cain, and Susanne Stemmer[b]
Materials Department, University of California, Santa Barbara, California 93106-5050, USA

(Received 13 October 2015; accepted 26 December 2015; published online 28 January 2016)

High-mobility perovskite $BaSnO_3$ films are of significant interest as new wide bandgap semiconductors for power electronics, transparent conductors, and as high mobility channels for epitaxial integration with functional perovskites. Despite promising results for single crystals, high-mobility $BaSnO_3$ films have been challenging to grow. Here, we demonstrate a modified oxide molecular beam epitaxy (MBE) approach, which supplies pre-oxidized SnO_x. This technique addresses issues in the MBE of ternary stannates related to volatile SnO formation and enables growth of epitaxial, stoichiometric $BaSnO_3$. We demonstrate room temperature electron mobilities of 150 $cm^2\ V^{-1}\ s^{-1}$ in films grown on $PrScO_3$. The results open up a wide range of opportunities for future electronic devices. [http://dx.doi.org/10.1063/1.4939657]

Functional perovskite oxides may enable entirely new electronic device paradigms, ranging from negative capacitance[1] to charge amplification[2] in phase change devices.[3] A major challenge is the intrinsically poor charge carrier mobility of most perovskite oxides, typically no better than 1–10 $cm^2\ V^{-1}\ s^{-1}$ at room temperature. The charge carrier mobility enters and limits the figure of merit or performance metric of almost any electronic device application. The recent discovery[4,5] of room temperature mobilities of ~300 $cm^2\ V^{-1}\ s^{-1}$ in doped single crystals of La-doped $BaSnO_3$ has therefore generated tremendous excitement.[6] In combination with its wide bandgap (~3 eV[7]), this makes $BaSnO_3$ of immediate interest as a new transparent conducting oxide and as a wide bandgap semiconductor for power electronics. Furthermore, for the first time, it would be possible to integrate functional perovskite oxides, such as ferroelectrics or strongly correlated oxides, on a lattice- and symmetry-matched, high-mobility semiconductor.[6] In particular, the conduction band offsets between $BaSnO_3$ and many functional oxides promote charge transfer into the $BaSnO_3$,[8] allowing for its use as a high-mobility channel.

Electronic device applications require the growth of high-quality films of $BaSnO_3$ with low defect densities. $BaSnO_3$ thin films have been grown using high-energetic deposition techniques, such as sputtering[9] and pulsed laser deposition,[4,10–12] but achieving high mobilities has been challenging. The best reported film mobilities are <80 $cm^2\ V^{-1}\ s^{-1}$ at room temperature.[4] Molecular beam epitaxy (MBE) is a low energetic deposition technique and routinely produces the highest mobility semiconductor[13] and functional oxide films.[14] However, stoichiometry control in MBE of perovskite oxides can be challenging.[15] For stannates, volatile SnO formation is a known issue.[16] As will be shown here, SnO and Sn volatility becomes a challenge in MBE of perovskite stannates. A modified MBE technique, where we replace the commonly used Sn metal source with SnO_2, successfully addresses these issues and allows for the growth of epitaxial, stoichiometric La-doped $BaSnO_3$ thin films with room temperature mobilities as high as 150 $cm^2\ V^{-1}\ s^{-1}$, twice that of previously reported films.

[a]S. Raghavan and T. Schumann contributed equally to this work.
[b]Email: stemmer@mrl.ucsb.edu

Conventional oxide MBE uses evaporation of high-purity metals to supply the cations, provided that they have sufficient vapor pressures for reasonable growth rates. All metals in $BaSnO_3$ and $SrSnO_3$ have sufficient vapor pressures for MBE. For example, Sn is a low melting solid and beam equivalent pressures (BEPs) of 4×10^{-8} Torr are obtained at an effusion cell temperature of 1160 °C. This should be sufficient to obtain reasonable growth rates, but problems arise in the MBE of Sn-based oxides, as discussed in detail below.

High-purity elemental Ba, Sr, Sn (4N, Sigma Aldrich), and SnO_2 (4N, Strem Chemicals) were evaporated using solid source effusion cells, and activated oxygen was provided using an oxygen plasma source (RF power 300 W). La was co-evaporated from an effusion cell for n-type doping. Prior to the growths, the substrates were subjected to a 20 min oxygen plasma anneal at the growth temperature. The substrate temperature was monitored using an infrared pyrometer (Ircon modline-3). All growths were performed using oxygen plasma with a BEP of 1×10^{-5} Torr, and samples were cooled down under the same oxygen plasma conditions after growth. Fluxes from the effusion cells were calibrated using a beam flux monitor. Normally, the Ba (Sr) BEP was kept constant and the SnO_x (Sn) BEP was adjusted. For $BaSnO_3$ films grown using the SnO_2 source, a Ba BEP $\sim 8 \times 10^{-8}$ Torr and SnO_x BEP $\sim 5 \times 10^{-7}$ Torr resulted in a film growth rate of 32 nm/hr. Film thicknesses were calculated using Laue thickness fringes from the film peak and corroborated using x-ray reflectivity and transmission electron microscopy (TEM). Stoichiometric conditions were found by changing the relative cation flux ratios, while keeping the oxygen BEP constant, in combination with *in situ* monitoring of reflection high-energy electron diffraction (RHEED) patterns and *ex situ* lattice parameter measurements by high-resolution x-ray diffraction (XRD). The RHEED of films grown in highly Sn-rich or Sr(Ba)-rich regimes was spotty indicating rough surfaces. An intermediate regime of phase-pure $BaSnO_3$ films was found using XRD, along with streaky RHEED patterns of these films. For TEM studies, cross-sectional specimens were prepared using an FEI Helios dual beam focused ion beam microscope. Samples were imaged using an FEI Titan S/TEM operating at 300 kV. Electrical properties were measured after annealing in oxygen atmosphere at 900 °C for 10 min to suppress oxygen vacancies. 50 nm Ti/300 nm Au Ohmic contacts were deposited using electron beam deposition after the annealing. Sheet carrier densities and Hall mobilities were measured in van der Pauw geometry using a Physical Property Measurement System (Quantum Design PPMS) from 300 K down to 4 K.

Figure 1(a) shows RHEED patterns recorded during MBE of a $SrSnO_3$ film on (001)$SrTiO_3$ at a substrate temperature of 550 °C, using only elemental metal sources and an oxygen plasma. Although XRD (Fig. S1 of the supplementary material[17]) indicates single-phase perovskite $SrSnO_3$, the RHEED pattern from the substrate completely disappears as soon as the Sr, Sn, and oxygen plasma shutters are opened. It reappears during growth (in this case after 30 min) but remains spotty

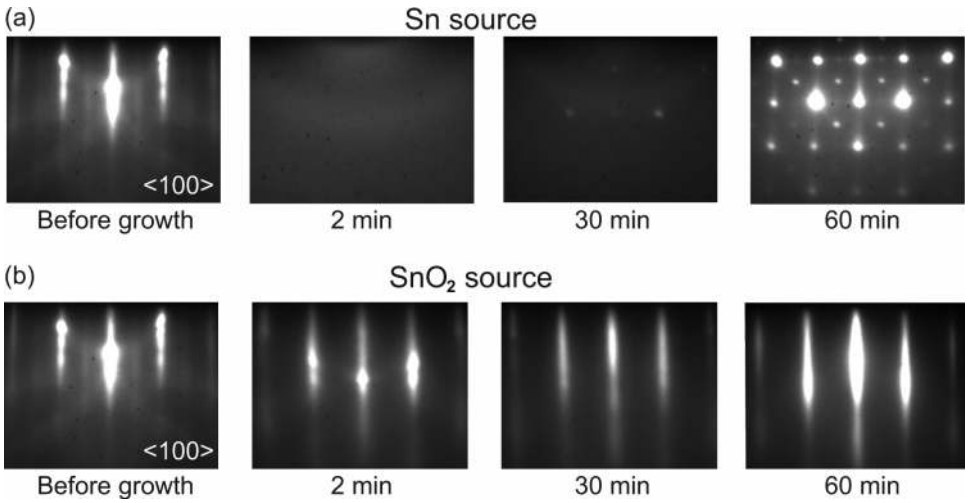

FIG. 1. RHEED patterns during growth on (001)$SrTiO_3$ of (a) $SrSnO_3$ using a Sn metal source at a substrate temperature of 550 °C and (b) $BaSnO_3$ using a SnO_2 source at a substrate temperature of 800 °C.

until the end (60 min), indicating three-dimensional growth. The most likely explanation for the initial RHEED is the formation of a layer of Sn metal droplets on the substrate. Sn metal droplets are a common issue in MBE of SnO_2 from a Sn metal source that has been well documented.[18] TEM (Fig. S2 of the supplementary material[17]) shows a defective interface layer that is likely a result of the initial Sn droplets. These droplets are an indication that volatile SnO consumes all active oxygen in the growth environment, leaving behind Sn.[18] To avoid SnO evaporation, the oxygen flux must either be increased or more reactive oxygen species (i.e., ozone) introduced. This would risk oxidation of filaments and other parts of the MBE system. More importantly, the growth of high quality perovskite films requires high substrate temperatures to achieve sufficient ad-atom mobility, typically in the range of 800–900 °C. Growths at higher substrate temperatures (above 550 °C) avoided the droplets, but causes excessive evaporation of Sn, as has also been observed in MBE of SnO_2.[16,18] In this study, no Sn incorporation was seen above 600 °C, and only SrO was deposited.

To address these issues, we adopted a modified MBE approach, namely, supplying pre-oxidized Sn from a SnO_2 source. There are only a few studies in the oxide MBE literature using evaporation of the metal oxide from an effusion cell.[19–23] Vapor pressure data indicate that SnO_2 sublimes in the form of suboxides (SnO_x) with vapor pressures sufficient for reasonable flux rates at practically feasible effusion cell temperatures, i.e., $\sim 10^{-5}$ Torr at 1300 °C.[24] Figure 1(b) shows RHEED during $BaSnO_3$ growth on (001)$SrTiO_3$ at a substrate temperature of 800 °C, using the SnO_2 source. The RHEED pattern is streaky from the start of the growth and remains so throughout, without any significant decrease in the intensity. This indicates that the surface of the $BaSnO_3$ film remains smooth. Supplying pre-oxidized Sn in the form of SnO_x in the presence of activated oxygen thus allows for the growth of epitaxial, stoichiometric, high-quality $BaSnO_3$, as discussed next.

Figure 2 shows structural data of $BaSnO_3$ grown on cubic (001)$SrTiO_3$ and orthorhombic (110)$PrScO_3$, respectively, using the SnO_2 source. Figure 2(a) shows an on-axis high-resolution

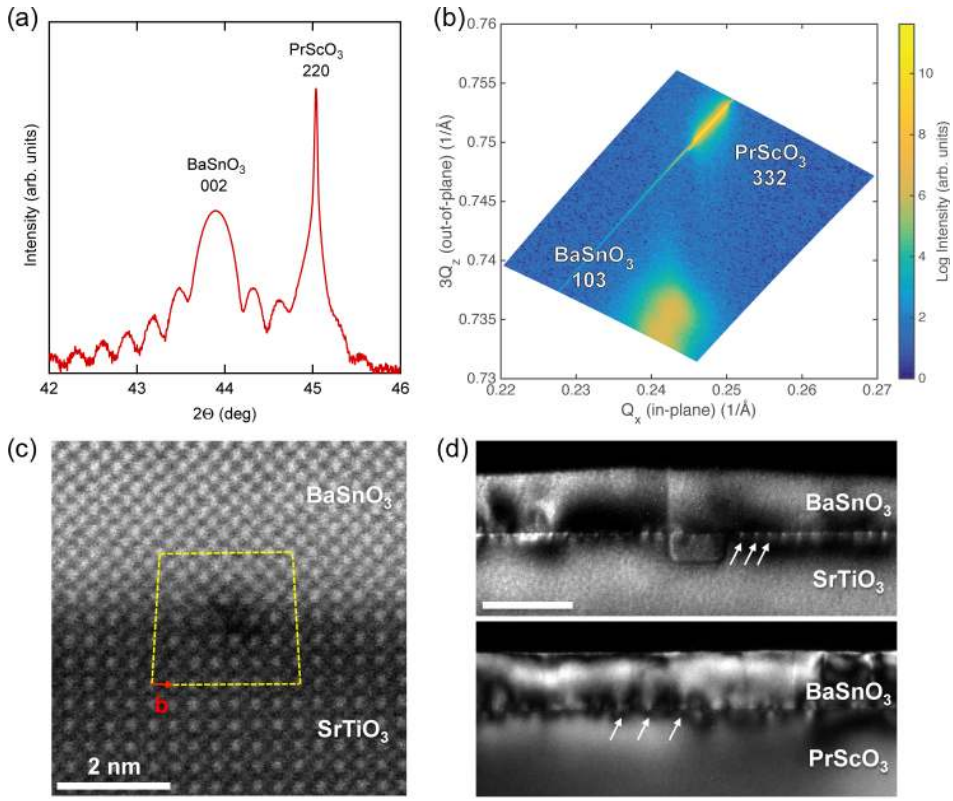

FIG. 2. (a) On-axis XRD around the 220 substrate reflection and (b) an asymmetric reciprocal space map around the 332 substrate reflection, for a 32 nm $BaSnO_3$ film on (110)$PrScO_3$. (c) HAADF-STEM image of a misfit dislocation at the $BaSnO_3$/$SrTiO_3$ interface with a Burgers circuit identifying the Burgers vector as a[100]. (d) Cross section dark-field TEM images of $BaSnO_3$ on $SrTiO_3$ (top) and $PrScO_3$ (bottom), showing misfit dislocations (white arrows).

XRD spectrum around the 002 peak of a 32 nm thick $BaSnO_3$ film on (110)$PrScO_3$. Wide-range x-ray scans show only $BaSnO_3$ and substrate peaks under stoichiometric growth conditions. Laue thickness fringes are present, indicating high structural quality and smooth interfaces. They are also obtained for $BaSnO_3$ on $SrTiO_3$ (see Fig. S3 of the supplementary material[17]). On $SrTiO_3$, the out-of-plane lattice parameter is 4.118 Å, close to the bulk value, indicating a stoichiometric and fully relaxed film, as expected given that the −5.4% lattice mismatch. On $PrScO_3$, which has an approximately −2.18% lattice mismatch, an out-of-plane lattice parameter of 4.117 Å is obtained for similar growth conditions. Figure 2(b) shows a reciprocal space map near the asymmetric 103 $BaSnO_3$ peak along with the 332 $PrScO_3$ peak. The in-plane lattice parameter of the film is 4.102 Å, slightly smaller than the bulk value, indicating a small in-plane strain (−0.3%) and an almost fully relaxed film.

Figures 2(c) and 2(d) show high-angle annular dark-field scanning transmission electron microscopy (HAADF-STEM) and diffraction contrast dark-field TEM images from cross section samples. Periodic misfit dislocations are seen at the interface [see arrows in Fig. 2(d)]. Their spacing is ∼8 nm on $SrTiO_3$, the expected value for a fully relaxed film. On $PrScO_3$, the spacing ranged between 20 and 30 nm, consistent with a partially relaxed film. The Burgers circuit is indicated around a misfit dislocation at the $BaSnO_3/SrTiO_3$ interface in Fig. 2(c).

Figure 3(a) shows the carrier mobility (μ) at 300 K as a function of carrier density (n_{3D}) for La-doped $BaSnO_3$ grown by MBE in this study and the best reported values from the literature. On $SrTiO_3$, μ of the ∼30 nm thick MBE films is ∼100 $cm^2\ V^{-1}\ s^{-1}$, which is 43% higher than that of the best films grown by other methods on the same substrate. It increases to ∼124 $cm^2\ V^{-1}\ s^{-1}$ for 64 nm thick films, most likely due to a reduction in scattering from the interface and/or some reduction in the threading dislocation density. On $PrScO_3$, μ of the ∼30 nm thick MBE films reaches 150 $cm^2\ V^{-1}\ s^{-1}$, approximately twice the value of any film in the literature. Figures 3(b) and 3(c) illustrate the temperature dependence of the transport properties on $SrTiO_3$ and $PrScO_3$, respectively. The carrier density in the two films is similar and almost independent of temperature, indicating minimal charge trapping at least at this doping level. Both films show metallic behavior, indicating that the films are degenerately doped, similar to the bulk crystals reported in the literature. μ approximately doubles between 300 and 4 K and begins to saturate below 100 K, when it becomes limited by ionized dopant and other defect-related scattering mechanisms. Noteworthy is the nearly 1:1 correspondence between lattice mismatch and μ at low temperature: reducing the mismatch by a factor of two increases μ by a similar factor. This signifies that the high defect densities introduced by the large lattice mismatch limit the transport properties on both substrates. As previously suggested for bulk crystals,[4] the high defect densities explain the need for high doping,

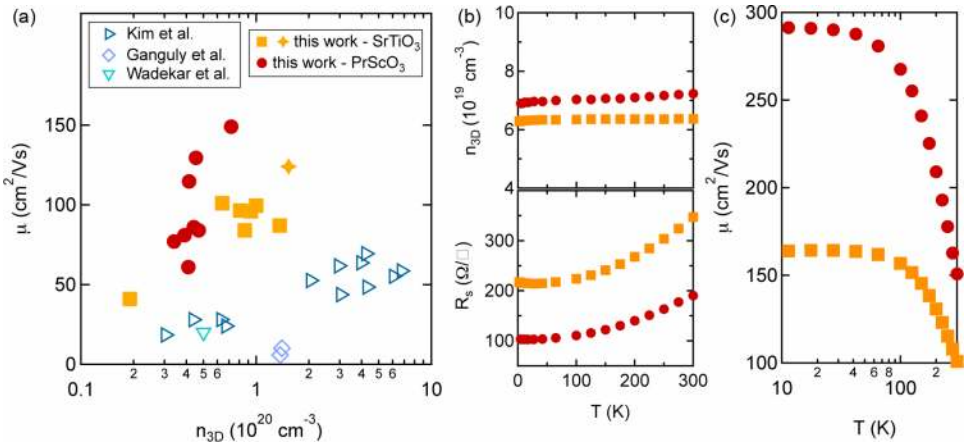

FIG. 3. (a) μ at 300 K as a function of n_{3D} for $BaSnO_3$ films grown on $SrTiO_3$ and $PrScO_3$ using oxide MBE (this work), and from reports from the literature (Kim *et al.*,[12] Ganguly *et al.*,[9] and Wadekar *et al.*[11]). The thickness of all films is 32 nm, except for one film on $SrTiO_3$ (starred), which was 64 nm. (b) Carrier density n_{3D}, sheet resistance R_s, and (c) mobility μ as a function of temperature T for $BaSnO_3$ films on $SrTiO_3$ (orange squares) and on $PrScO_3$ (red dots), respectively.

which assists in screening the defects. Nevertheless, the high room temperature mobility of these films should already enable many of the applications discussed above.

In summary, we have shown that a modified MBE approach, which uses sublimation from a SnO_2 source, enables MBE of high-quality $BaSnO_3$ films with room temperature mobilities of 150 $cm^2\ V^{-1}\ s^{-1}$, twice as a high as by any other method. Similar to MBE of $SrTiO_3$[25,26] and other complex oxides,[14] these results emphasize the importance of stoichiometry control and the use of a low energetic deposition technique in attaining high quality perovskite films. The results furthermore show that mobilities can likely be increased further by the development of substrates with lower mismatch. In addition to $BaSnO_3$ itself (currently only small flux grown needles have been reported[6]), several candidates exist[27] but are not commercially available yet. An alternative approach would be to grow on relaxed buffer layers, similar to what is used in GaN-based technologies. MBE of $BaSnO_3$ thus lays the path for numerous potential applications in oxide electronics requiring high-mobility channels.

Note added in proof. After the submission of this manuscript, another study reporting MBE of $BaSnO_3$ films was published in Ref. 28. No electrical data was reported.

Film growth experiments and electrical measurements were supported by the US National Science Foundation (Grant No. DMR-1409985) and the Extreme Electron Concentration Devices (EXEDE) MURI of the Office of Naval Research (ONR) through Grant No. N00014-12-1-0976. The TEM experiments were supported by the US Department of Energy (Grant No. DEFG02-02ER45994) and the UCSB MRL, which is supported by the MRSEC Program of the US National Science Foundation under Award No. DMR 1121053.

[1] S. Salahuddin and S. Datta, Nano Lett. **8**, 405 (2008).
[2] J. Son, S. Rajan, S. Stemmer, and S. J. Allen, J. Appl. Phys. **110**, 084503 (2011).
[3] C. H. Ahn, A. Bhattacharya, M. Di Ventra, J. N. Eckstein, C. D. Frisbie, M. E. Gershenson, A. M. Goldman, I. H. Inoue, J. Mannhart, A. J. Millis *et al.*, Rev. Mod. Phys. **78**, 1185 (2006).
[4] H. J. Kim, U. Kim, H. M. Kim, T. H. Kim, H. S. Mun, B.-G. Jeon, K. T. Hong, W.-J. Lee, C. Ju, K. Hoon Kim *et al.*, Appl. Phys. Express. **5**, 061102 (2012).
[5] X. Luo, Y. S. Oh, A. Sirenko, P. Gao, T. A. Tyson, K. Char, and S. W. Cheong, Appl. Phys. Lett. **100**, 172112 (2012).
[6] S. Ismail-Beigi, F. J. Walker, S. W. Cheong, K. M. Rabe, and C. H. Ahn, APL Mater. **3**, 062510 (2015).
[7] H. Mizoguchi, H. W. Eng, and P. M. Woodward, Inorg. Chem. **43**, 1667 (2004).
[8] L. Bjaalie, B. Himmetoglu, L. Weston, A. Janotti, and C. G. Van de Walle, New J. Phys. **16**, 025005 (2014).
[9] K. Ganguly, P. Ambwani, P. Xu, J. S. Jeong, K. A. Mkhoyan, C. Leighton, and B. Jalan, APL Mater. **3**, 062509 (2015).
[10] S. Sallis, D. O. Scanlon, S. C. Chae, N. F. Quackenbush, D. A. Fischer, J. C. Woicik, J. H. Guo, S. W. Cheong, and L. F. J. Piper, Appl. Phys. Lett. **103**, 042105 (2013).
[11] P. V. Wadekar, J. Alaria, M. O'Sullivan, N. L. O. Flack, T. D. Manning, L. J. Phillips, K. Durose, O. Lozano, S. Lucas, J. B. Claridge *et al.*, Appl. Phys. Lett. **105**, 052104 (2014).
[12] H. J. Kim, U. Kim, T. H. Kim, J. Kim, H. M. Kim, B. G. Jeon, W. J. Lee, H. S. Mun, K. T. Hong, J. Yu *et al.*, Phys. Rev. B **86**, 165205 (2012).
[13] L. Pfeiffer and K. W. West, Physica E **20**, 57 (2003).
[14] D. G. Schlom, APL Mater. **3**, 062403 (2015).
[15] D. G. Schlom, J. H. Haeni, J. Lettieri, C. D. Theis, W. Tian, J. C. Jiang, and X. Q. Pan, Mater. Sci. Eng.: B **87**, 282 (2001).
[16] M. E. White, M. Y. Tsai, F. Wu, and J. S. Speck, J. Vac. Sci. Technol., A **26**, 1300 (2008).
[17] See supplementary material at http://dx.doi.org/10.1063/1.4939657 for high-resolution XRD of a $SrSnO_3$ film grown using a Sn source, a cross section TEM image of the film, and high-resolution XRD of a $BaSnO_3$ film grown on $SrTiO_3$ using a SnO_2 source.
[18] M. Y. Tsai, M. E. White, and J. S. Speck, J. Appl. Phys. **106**, 024911 (2009).
[19] O. Bierwagen, A. Proessdorf, M. Niehle, F. Grosse, A. Trampert, and M. Klingsporn, Cryst. Growth Des. **13**, 3645–3650 (2013).
[20] T. Watahiki, W. Braun, and H. Riechert, J. Vac. Sci. Technol., B **27**, 262 (2009).
[21] K. Sasaki, A. Kuramata, T. Masui, E. G. Vıllora, K. Shimamura, and S. Yamakoshi, Appl. Phys. Express **5**, 035502 (2012).
[22] Z. Galazka, R. Uecker, D. Klimm, K. Irmscher, M. Pietsch, R. Schewski, M. Albrecht, A. Kwasniewski, S. Ganschow, D. Schulz *et al.*, Phys. Status Solidi A **211**, 66 (2013).
[23] P. Vogt and O. Bierwagen, Appl. Phys. Lett. **106**, 081910 (2015).
[24] R. H. Lamoreaux, D. L. Hildenbrand, and L. Brewer, J. Phys. Chem. Ref. Data **16**, 419 (1987).
[25] J. Son, P. Moetakef, B. Jalan, O. Bierwagen, N. J. Wright, R. Engel-Herbert, and S. Stemmer, Nat. Mater. **9**, 482 (2010).
[26] T. A. Cain, A. P. Kajdos, and S. Stemmer, Appl. Phys. Lett. **102**, 182101 (2013).
[27] F. S. Galasso, *Perovskites and High T_c Superconductors* (Gordon and Breach Science Publishers, New York, 1990).
[28] A. Prakash, J. Dewey, H. Yun, J. S. Jeong, K. A. Mkhoyan, and B. Jalan, J. Vac. Sci. Technol. A **33**, 060608 (2015).